Directionality and community-level selection

Guy Bunin

Department of Physics, Technion-Israel Institute of Technology, Haifa 32000, Israel

We study models of ecological community dynamics, in which each species is in mutually-exclusive competition with a number of other species. We find that at high enough diversity the dynamics are directional, meaning that the community state can be characterized by a function that increases in time. In contrast to dynamics that exhibit directionality by construction, this constitutes a novel property of emergent directionality. It stems purely from strong competitive interactions, and may therefore be more robust and general. In the presence of noise, the directionality drives the system to ever more stable states, with production increasing over long times. When a spatial dimension is added, in the form of a meta-community comprised of multiple coupled communities, community states with higher values of this function are able to expand in space, forming (exact or approximate) copies of themselves. This leads to community-level selection with the same function acting as a fitness.

A wide range of spatio-temporal patterns in ecological communities exhibit some degree of directionality and predictability, and are studied collectively under the name of succession patterns [1].

Yet, directionality in the dynamics of many interacting species is all but a given. Some communities, from bacteria to forests, exhibit stochastic [2] and chaotic [3] changes in dominance. Complex and non-directional dynamics, from cycles to chaos, are found in many-species dynamical models in ecology [4,5], and in related models in evolution [6] and game theory [7,8]. Intuitive mechanisms for directionality often require strong hierarchies or fine-tuned trade-offs between species, that might not emerge in a high-dimensional space of traits and interactions [9].

In this work, we show that it is theoretically possible for collectives of species to exhibit directed dynamics, both in their local succession and in their spatial expansion. Within a well-mixed community, we show how directionality emerges under certain conditions and at sufficiently high diversity (tens of species). This directionality contributes to the stability of certain states, out of the many alternative states available to the system.

Once a spatial dimension is introduced, these stable states act as a new level of organization, and are able to expand to neighboring locations. Moreover, states favored by the local directionality also expand more efficiently in space. To describe the spatial dynamics, concepts from evolutionary dynamics provide a powerful analogy. Even though all the mechanisms involved are strictly ecological (specifically, species' interactions and migration), states that expand efficiently in space can take over the ecosystem, in analogy with the way that high-fitness genotypes (or phenotypes) are selected for in evolutionary population dynamics. Thus, directionality may be enhanced by the spatial dimension through a community-level selection process.

Many different scenarios for directionality, and related maximum principles, have been proposed and continue to be debated [10]. Some models are directional by construction. For example certain resource competition models [11,12], but not others [4]. Here, in contrast, directionality is not imposed and stems purely from the effect of strong competitive interactions at sufficiently high diversity. It may therefore be more robust and general. Its applicability to a given system can be determined with little knowledge on the underlying mechanisms that generate the interactions.

The notion of the community as an important level of organization dates back to the early days of succession theory [13], and informs our current understanding of associations of organisms from different species [14], such as host-microbe interactions [15,16]. In dynamical models, the effect of externally imposed community selection was studied in [17], and the effect of host replication on microbe communities was studied in [16]. In coalescence simulations, communities display a degree of cohesiveness. In [18] the outcome of community coalescence was shown to be similar to one of the two initial communities. In [19], coalescence was studied in a resource-competition model whose dynamics are directional. The fate of individual species was shown to be better predicted by the dynamically increasing (Lyapunov) function of the original community, than by a single-species fitness measure. Spatial expansion of one stable state into another one has been studied in general models of bistability, and in more detailed accounts of specific transitions [20–25]. Much less is known about the long-term behavior of spatially extended systems with a large number of alternative states.

The family of models discussed below admits many alternative stable equilibria, a property that can emerge

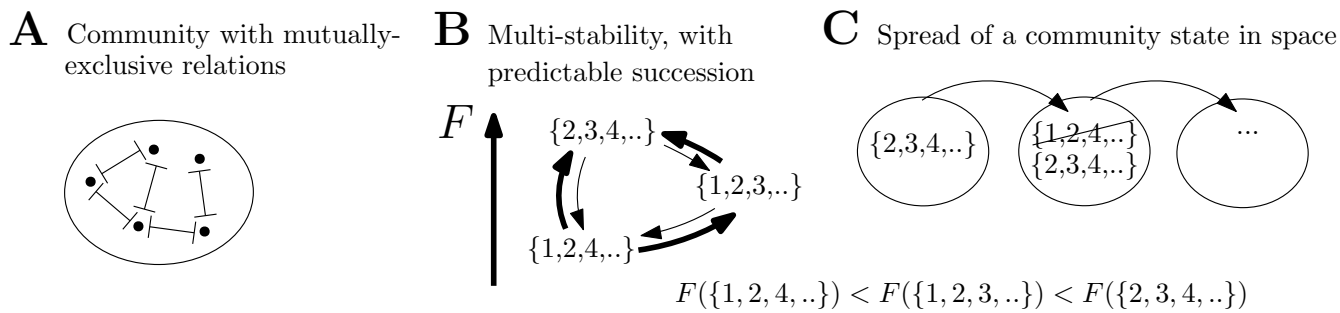

Figure 1: (A) Illustration of a community in which some pairs of species are mutually exclusive (marked by $\vdash\!\dashv$ symbols). Other interactions may also exist. (B) A known function (F) of the community imposes directionality in the dynamics of the system. The ecological community exhibits multiple alternative states (each indicated by the list of its established species). The state may change in the time, with a tendency to transition towards states with higher values of F (thicker arrows show the more likely transitions). (C) When multiple local communities are coupled by migration, certain states are found to expand across the different communities. States with higher values of F tend to expand more efficiently.

in different ways at high diversity [7, 26–29]. The scenario described in [28, 29] is the most relevant to the present work. Directionality in the presence of many equilibria has been studied for various dynamics across scientific fields, and often found to require certain fine-tuned trade-offs [7,27,30–32]; as shown below, this is not the case in the present model.

The paper is structured as follows: Sec. 1 describes the model for a single community of interacting species without spatial structure. We introduce the essential ingredient of the model, the existence of pairs of species which are mutually exclusive–namely, in which either of the species can prevent the other from invading–see Fig. 1(A). Mutual exclusion is expected theoretically and measured in many situations, e.g., [33–37]. Beyond this property the behavior is insensitive to many modeling details and does not require fine-tuning of parameters.

Sec. 2,3,4, discuss how directionality emerges at sufficiently high species diversity, and describe the function that increases in time, see Fig. 1(B). The same function increases also in the presence of noise, as the system moves between multiple alternative states, exploring ever more stable, longer lasting states. The ecological interpretation of this function and its relation to growth in production are discussed.

In Sec. 5, insight into these phenomena is obtained from a simple instance of the general model, with just 3 species. Spatial structure is then added to the model, realized as a meta-community, in which multiple communities are coupled by migration. The simple model demonstrates some of the phenomena that appear in high-diversity cases: that states may expand in space and that the same function that increases in a local community is also associated with better ability to replicate, and thus acts as a fitness function, see Fig. 1(C). This contributes to directionality by selection of higher values of the function, in analogy with the increase of fitness in population dynamics. In Sec. 6, these results are then shown to hold and generalize to the full, high-diversity spatial model. Sec. 7 discusses the generality and limitations of the model, followed by a discussion in Sec. 8.

1 Model definition

Here a single, well-mixed community is discussed, with spatial structure left for later sections. We describe an ecological community, with predominantly competitive interactions, where every species is, on average, *mutually exclusive* with a few other species. By this we mean that if these two species are mixed, a stable equilibrium will contain one or the other species, but not both. Many model variants will give similar results, for concreteness we focus on the usual Lotka-Volterra model for the relative abundances (yields) of S species, $N_{i=1..S}$,

$$\frac{dN_i}{dt} = r_i N_i \left(1 - \sum_{j=1}^{S} \alpha_{ij} N_j\right) + \lambda_i + \omega_i \sqrt{N_i}\eta_i \ , \quad (1)$$

with $\alpha_{ii} = 1$. The λ_i term accounts for migration. In the demographic noise term, $\omega_i\sqrt{N_i}\eta_i$, $\eta_i(t)$ is white noise and ω_i is related to the absolute number of individuals of each species.

As mentioned above, the main property relevant below is whether there exist pairs of species that are mutually exclusive. In Eq. (1) this translates to a pair i, j for which both $\alpha_{ij}, \alpha_{ji} > 1$. In the following, the matrix α is taken be sparse and, motivated by niche theory

where species interact when their niches overlap, it is assumed that α_{ij}, α_{ji} are either both non-zero or both zero. α_{ij}, α_{ji} are *not* assumed to be equal or similar in their values. Each species interacts with C other species. Additional model parameters are given in the following sections; many variations on this basic model and its assumptions give similar results, see Sec. 7.

2 Directionality and stability in a multi-stable setting

In this section we show how directionality emerges in many-species dynamics, in the presence of strong competition. Directionality can be imposed in the structure of the model, as in certain resource competition models [11, 12], or through specific model constraints as discussed below. Here we show that, even if it is not imposed by construction, directionality can emerge dynamically provided that interactions are sufficiently competitive.

We first consider the noiseless case, i.e. setting all $\omega_i = 0$. When the matrix A with $A_{ij} \equiv r_i \alpha_{ij}$ is symmetric it is well known (e.g., [38]) that the function

$$F(t) = 2\sum_{i=1}^{S} r_i N_i(t) - \sum_{i,j=1}^{S} r_i \alpha_{ij} N_i(t) N_j(t) \quad (2)$$

is non-decreasing during the dynamics of Eq. (1) without noise. Such a function is known as a Lyapunov function. However if A is not symmetric[1] F may generally decrease during the dynamics. Let's look at what happens in this more general case.

Fig. 2(A), shows runs with different values of mean (α_{ij}), the mean of all non-zero interactions, keeping all other parameters constant (parameters are given in Appendix A). When mean (α_{ij}) is small enough such that most interactions satisfy $\alpha_{ij} < 1$, $F(t)$ first increases and then fluctuates indefinitely, indicating that the abundances fluctuate, and the dynamics do not reach a fixed point[2]. Increasing mean (α_{ij}), we see that systems are more likely to converge to fixed points, after some oscillations of the function $F(t)$. Increasing the mean further, so that for a large fraction of the non-zero interactions $\alpha_{ij} > 1$, the function $F(t)$ *increases throughout the entire dynamics*, and always converges to

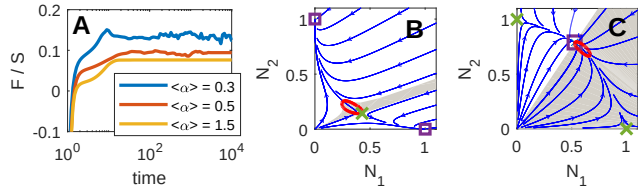

Figure 2: Directionality can emerge, even if not imposed by construction. (A) The function $F(t)$ in a system with many species, for three different runs. In each run the mean value of the non-zero α_{ij} is different, with other parameters kept constant. As the mean is increased, the behavior changes from persistent fluctuations in $F(t)$ and dynamics that do not reach a fixed point, to dynamics in which $F(t)$ only increases until equilibrium. Comparison between mutual-exclusion (B) and coexistence (C) for $S = 2$, gives an idea for the reasons for the growth of F. $F(t)$ decreases when entering the areas delineated in red, which happens for dynamics initialized anywhere in the gray regions. Squares and crosses mark stable and unstable fixed-points, respectively. In (A), each species interact with $C = 20$ other species, and $S = 400$.

a fixed point[3]. In other words, $F(t)$ behaves as if it were a Lyapunov function.

Why does $F(t)$ increase under these conditions? Roughly speaking, the decrease of $F(t)$ comes from pairs of species that compete and are sufficiently abundant, a combination that is precluded by mutual-exclusion. To illustrate the point, we look at a model with just two species. A two-species system with mutually-exclusive interactions, i.e. where both $\alpha_{12}, \alpha_{21} > 1$, is bi-stable and has a third unstable fixed point, see Fig. 2(B). The area in phase space where F decreases along the dynamics is close to the *unstable* fixed point. In contrast, when the two species may coexist in equilibrium, $\alpha_{12}, \alpha_{21} < 1$, Fig. 2(C), this area is close to the stable fixed point. This difference means that in the case of coexistence, trajectories starting from random initial conditions are likely to pass through this region, while in the bi-stable case, trajectories are more likely to avoid this region. In models with higher S, the number of terms in F grows, and regions where F decreases become more and more rare, with a small fraction of the trajectories passing through a region with decreasing $F(t)$. This argument is of course not a proof, and more work is needed to understand this result. This directionality happens at rather small values of S: for a model sampled as described in the beginning of Sec. 3, F decreases in only $16\%_{(\pm 2\%)}$ of the runs with $S = 4$ and $1\%_{(\pm 1\%)}$ of the

[1] To admit a Lyapunov function, the matrix A can be of a somewhat more general form than symmetric [38]. The model described below does not satisfy this form.

[2] This behavior depends on the parameter $\sigma = \sqrt{C}\,\mathrm{std}(\alpha_{ij}) / [1 - \mathrm{mean}(\alpha_{ij})]$ [26, 27], which diverges at mean $(\alpha_{ij}) = 1$. A transition to stable equilibria has also been reported in simulations of [39].

[3] In some runs with $\langle \alpha_{ij} \rangle = 1.5$ there may be a small decrease in F, with minimal dF/dt of order -10^{-5}. This small effect is suppressed when $\langle \alpha_{ij} \rangle$ is higher (say, $\langle \alpha_{ij} \rangle = 2$) and λ smaller.

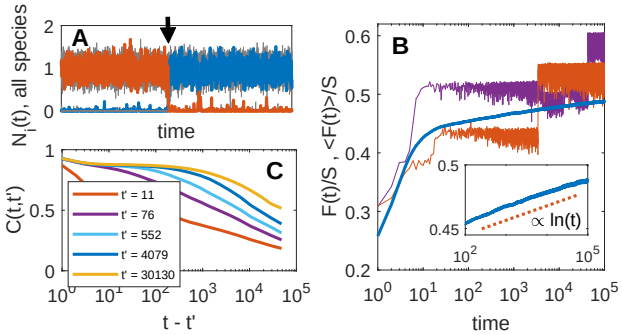

Figure 3: The dynamics with noise. (A) Each species is either found at very low abundance maintained only by migration, or is established. The system may undergo noise-driven changes of state, as in the simple one marked by an arrow, where one established species is replaced by another. (B) The function $F(t)$ in two example runs (thin lines), and the mean over many runs (thick line). Inset: close up on the mean $\langle F(t)\rangle$ at later times ($t > 100$), showing its continued growth. (C) The correlation function between two times t' and t decays more slowly as t' grows, showing that the dynamics slow down as more stable states are explored. Here and in Figs. 4,6, each species interacts with $C = 3$ other species, and $S = 24$.

runs with $S = 8$.

3 Noise and slowing-down of the dynamics

In the presence of noise the system may switch between otherwise stable states. The term 'state' refers to a stable equilibrium together with its basin of attraction under noiseless dynamics. Fig. 3 shows results for noisy dynamics. Here and in Sec. 4,6, the species pool has $S = 24$ species, each interacts with $C = 3$ other species, and the non-zero α_{ij} are sampled from a Gaussian distribution with $\text{mean}(\alpha_{ij}) = 1.667$ and $\text{std}(\alpha_{ij}) = 0.75$. With these parameters, the community occupies a single trophic level, where all species pairs are either competitive ($\alpha_{ij} > 0$) or do not interact. Other parameters are given in Appendix A.

Fig. 3(A) shows an example of a transition in the composition of species, where one species is able to invade at the expense of another which is removed from the community. As expected, $F(t)$ fluctuates due to the noise; remarkably it tends to *increase* in time. It is shown in Fig. 3(B) for two example trajectories. At long times, $t \gtrsim 100$, $F(t)$ shows periods of fluctuations within a single state, punctuated by abrupt transitions in which $F(t)$ more often increases than decreases. The mean of $F(t)$ over many runs increases at long times roughly as $\langle F(t)\rangle \sim \ln t$, see Fig. 3(B). The angular brackets $\langle ..\rangle$ denote average over samples of the interactions, growth rates, initial conditions and noise. This growth at long times is a non-trivial behavior, which is not found in many other models or parameter regimes, such as when noise is added to the chaotic regime discussed above, causing $\langle F(t)\rangle$ to quickly reach a plateau, see Appendix B.

With time, the dynamics slow down, spending longer periods of time in one state, as can be appreciated from the runs shown in Fig. 3(B) (note the logarithmic scale in the time axis). To quantify whether the state has changed, and if so by how much, we look at the correlation function $C(t, t')$, measuring the similarity (correlation coefficient) between the abundances $N_i(t')$ and $N_i(t)$, with $t' < t$. Fig. 3(C) shows that at later times t', the correlation decays more slowly with $t - t'$, reflecting a *growth in stability*, in the sense that the system spends ever longer times in any given state or in states similar to it[4]. Thus, states with larger F are also more stable.

The transitions between states appear as jumps in Fig. 3(A,B), demonstrating that the system has multiple equilibria. There are various ways in which a highly-diverse community may admit multiple-equilibria [7,26–29], resulting in different organizational and dynamical properties. The structure of equilibria in communities whose interactions are predominately mutually-exclusive has been studied in [28,29]. In this setting, a stable equilibrium is comprised of a set of species which do not exclude each other, and to which no additional species can be added. One then finds multiple equilibria, and for large systems very many of them – exponentially many in the number of species S [28].

The bias towards higher F in the dynamics provides a simple mechanism for the growth in stability, as transitions are biased towards states with higher F, so that states with large F have less such states to switch to. This also helps to slow down the rate of change, as seen in the correlation functions.

4 Interpretation of $F(t)$ and growth of production

Over longer times, the changes in $F(t)$ slow down. When the changes are slow, $F(t)$ is approximately equal to an alternative and more suggestive form [43].

[4] This is in contrast with simple models of multi-stability which only contain two (or a handful) of alternative states [40], where $C(t, t')$ would depend only on the time difference $t - t'$, decaying after the time typical to the jump between these states. The behavior observed in the present model is characteristic of dynamics

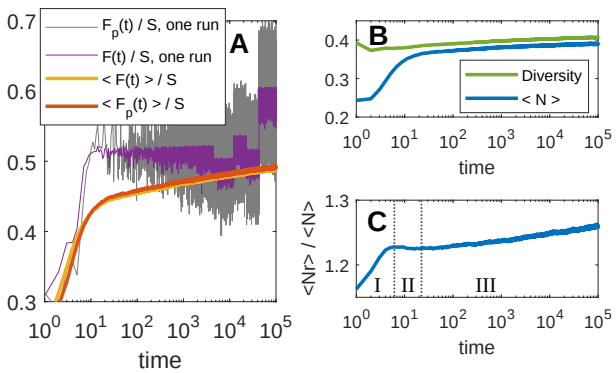

Figure 4: Growth of production. (A) Comparison of $F(t)$ and $F_p(t)$. Over one run (thin lines), they fluctuate around the same values, with $F_p(t)$ showing larger fluctuations. The averages over many runs match well. (B) Over long times, the diversity grows (the fraction of established species, $N_i > 0.25$, see Fig. 3(A)), as does the average abundance. Apparent early decline in diversity comes before first state stabilizes (see also Fig. 6(D)), at which times the diversity criteria for isn't relevant. (C) Mean per capita growth rate, showing three periods: I. colonization (increase of function); II. maturation within state (saturation and some decrease); III. jumps between states (increase, again).

When the dynamics slow down, and after averaging out the rapid fluctuations due to the noise, changes in the total biomass are small, $\frac{d}{dt}\left(\sum_{i=1}^{S} N_i\right) \simeq 0$. Eq. (1) becomes

$$0 \simeq \sum_{i=1}^{S} \frac{dN_i}{dt} = \sum_{i=1}^{S} r_i N_i (1 - \sum_{j=1}^{S} \alpha_{ij} N_j) \ ,$$

where migration is assumed to be negligibly small. Rearranging and using Eq. (2) we find at long times

$$F(t) \simeq F_p(t) \equiv \sum_{i=1}^{S} r_i N_i(t) \ . \tag{3}$$

The expression for $F_p(t)$ in Eq. (3) is simply the average over bare growth rates r_i, weighted by the abundances $N_i(t)$. It is thus a form of production [43] - it would be equal to the total biomass production if the growth rates corresponded to the per-capita biomass production, and weighted by the biomass. As shown in Fig. 4(A), $F_p(t)$ and $F(t)$ both fluctuate around a common average, which moves upon transitions between states. The averages over many realizations of the model, $\langle F_p(t)\rangle, \langle F(t)\rangle$, match closely. $F(t)$ can be seen to fluctuate less than $F_p(t)$ in Fig. 4(A), since $F(t)$ fluctuates around a local maximum, while $F_p(t)$ is a simple linear function of the abundances, which does not admit a local maxima at the equilibria. $F_p(t)$ does not generally increase when equilibria are approached, so while stability of states and the transitions between them are closely tied to the increase in $F(t)$, the increase in $F_p(t)$ is in a sense a by-product of the behavior of $F(t)$.

The function $F_p(t)$ can be split into the product of the change in the total abundance $\sum_i N_i(t)$ and the weighted average of the growth rates, $\sum_i N_i r_i / \sum_i N_i$, which is akin to productivity [1] (biomass production per unit biomass). In simulations of the model, the later is found to have a characteristic shape, see Fig. 4(C): at very short times it grows rapidly, as species with large r_i increase in abundance in this colonization period. It then levels off and decreases a little. This saturation and decrease in productivity is known to occur during community maturation [1], as fast growing species (high r_i) are replaced with species that are able to coexist. At later times ($t \gtrsim 100$) the community transitions between different possible states. At this stage the diversity of the community, the average growth rate and the total abundance $\sum_i N_i$ all gradually increase, see Fig. 4(B). These can be related the growth of $F_p(t)$, with the growth of $\sum_i N_i r_i$ entailing that of averages of N_i and r_i. It might be more model dependent.

5 Stability, directionality and spatial expansion

To get some intuition on the growth in production F_p and stability in the presence of noise, we study a simple instance of the model. We then use it to introduce spatial structure, before adding spatial structure to the full, high-diversity case in the next section. The simple model features three species, "1", "2" and "3". Species 1 has mutual exclusive relations with 2 and 3, see Fig. 5, and species 2,3 have no direct interaction (they could interact sufficiently weakly without changing the results). In this situation there are two equilibria of the noiseless dynamics: one with species 1 present and 2,3 suppressed due to the mutual exclusive relations; and another with 2,3 present and 1 suppressed. They will be denoted by s_1 and s_{23} respectively. We take all $r_i = 1$, returning to that later.

With noise, the system fluctuates around one of the two equilibria, with occasional transitions between them, see Fig. 5(A). The F-values of the two equilibria can be readily calculated from Eq. (2) or Eq. (3), giving $F_1 = 1$ and $F_{23} = 2$. Therefore we expect the system to jump more easily from s_1 to s_{23} than in the opposite direction, and so spend more time in s_{23}. Indeed, with $\omega_i^2 = 0.1$

in complex high-dimensional landscapes [41, 42].

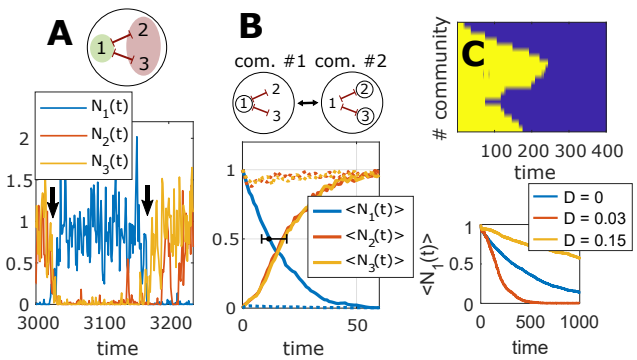

Figure 5: (A) A simple community, with three species (1,2,3) and two competitive-exclusion relations (marked by $\vdash\!\dashv$ symbols), with $\alpha_{ij} = \alpha_{ji} = 1.5$. This has two equilibria: one (s_1) with only species 1 present and 2,3 suppressed, and the other (s_{23}) with species 2,3 present, and 1 suppressed (colored ellipses). The system jumps more easily from the state s_1 to the state s_{23}. Both transitions are shown in an example run (marked by arrows). (B) When communities are coupled by migration, states can expand to neighboring communities. Here, two communities as in A are coupled, one initialized in state s_1 and the other in s_{23} (circled species). The state s_{23} rapidly takes over both communities. Shown are time averages over repeated runs, for community initialized in s_1 (solid lines) and in s_{23} (dotted lines). The horizontal errorbar shows the standard deviation in the time when N_1 crosses below 0.5. Migration rate is $D = 0.03$. (C) A chain of $M = 20$ coupled communities, all initialized in state s_1 (in yellow, defined by $N_1(t) > 0.25$). The state changes to s_{23} in two places, and expands to all the communities (here $D = 0.03$). Bottom: $\langle N_1(t)\rangle$ is shown for $M = 20$ and different D. The transition to s_{23} may be faster ($D = 0.03$ as in top panel) or slower ($D = 0.15$) than for a single community ($D = 0$). In all panels $\omega_i = 0.173$ for all species.

the system is at s_1 only about 7% of the time (measured by the fraction of time that $N_1(t) > N_2(t), N_3(t)$).

To understand the asymmetry in the transition rates, consider the transition processes. The system switches from s_1 when the abundance of N_1 is low enough, by some random fluctuation driven by the noise, so that either N_2 or N_3 grow from their low values, see the second transition in Fig. 5(A). Transitioning in the other direction requires both N_2 and N_3 to be unusually low simultaneously before N_1 can increase, see the first transition in Fig. 5(A). The latter transition is therefore less likely. This is a mechanism for growth in $\sum_i N_i$, representing higher total abundance or diversity: transitioning from high- to low-diversity requires more species to be unusually low simultaneously, than vice-versa.

If species have different growth rates, a preference for higher r-values comes from two mechanisms. First, species with higher r are more stable, with smaller noise-induced fluctuations. Secondly, upon transitioning, species with higher r-values grow faster, making transitions to states in which they are present more likely.

We now introduce spatial structure. Space is modeled within the meta-community framework, in which M communities are coupled by migration, and each community is well-mixed and subject to internal dynamics as in Eq. (1). Let $N_i^{(u)}$ be the abundance of the i-th species in the u-th community. The equations read

$$\frac{dN_i^{(u)}}{dt} = .. + \sum_{v\sim u} D_i^{(u,v)} \left[N_i^{(v)} - N_i^{(u)}\right] . \quad (4)$$

where the "..." refers to the terms in the RHS of Eq. (1), applied to $N_i^{(u)}$. In particular the small external migration term λ_i is kept in all communities, meaning that they are also weakly coupled to an external pool of species, so that all species can try to invade. Interactions α_{ij} and growth rates r_i are taken to be the same in all M communities. In the following we take all migration rates to be identical, $D = D_i^{(u,v)}$.

In Fig. 5(B), two communities are coupled by migration, with the interactions in each community as discussed above (Fig. 5(A)). The abundances are initialized with one community in equilibrium s_{23} and the other in s_1. Without noise and at sufficiently small migration rate D, this assignment of abundances is stable: each community is stable against the invasions via migration from the other community. However with noise, the state s_{23} is able to expand and take over both communities, see Fig. 5(B), which shows $\langle N_{1,2,3}(t)\rangle$ in the community initialized at s_1 (with $N_1 = 1, N_2 = N_3 = 0$ at $t = 0$), quickly transitioning to state s_{23}. The reason for the asymmetry in the transition is again that the takeover requires only one species to decrease in s_1, compared to two in the community with s_2, and migration from a neighboring community catalyzes the process.

Coupling more communities allows for spreading of a state throughout the meta-community. In Fig. 5(C), 20 communities are coupled in a linear chain, each to its two nearest neighbors. The dynamics in time and space are visualized in two dimensions, with the vertical axis showing the patches as ordered along the chain, and the horizontal axis corresponding to time. The system is initialized with all communities in state s_1. We see that state s_{23} eventually takes over. In the top example the switch first happens in two communities, and then spreads to the rest of the system via migration. This change happens faster in the meta-community than for a single community, see bottom panel.

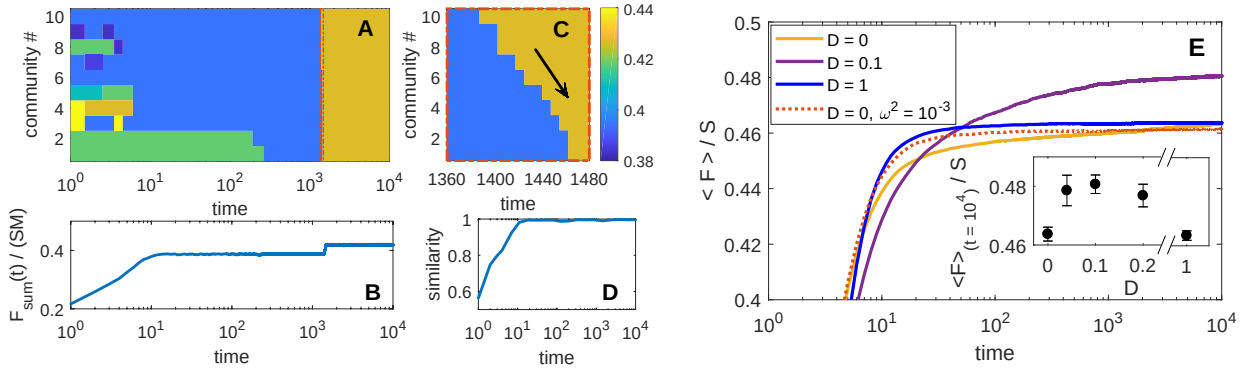

Figure 6: Meta-community dynamics. (A) An example run, showing the function F of the state in each community (defined as F of the equilibria reached by zero-noise dynamics of the patch in isolation). (B) Average of F over all the communities. (C) A close-up on a change in population state (narrow red rectangle in (A)). A new community state, first appearing in the top-most community, spreads until taking over the entire meta-community. The arrow shows the direction of the spread. (D) The similarity of the noisy state to the zero-noise equilibria, showing the initial dynamics towards an equilibrium, up to time $t \sim 10$. (E) The mean $\langle F(t) \rangle$ over all communities and many runs, for different migration rates D. Intermediate values ($D = 0.1$) allow $\langle F(t) \rangle$ to grow well above the value reached for a single community ($D = 0$). High migration rates ($D = 1$) suppress the growth of F at late times, and the system behaves as if it is well-mixed with smaller noise (dotted line). Inset: $\langle F \rangle$ at time $t = 10^4$, which depends non-monotonically on D. In all panels there are $M = 10$ communities, all $\omega_i = 0.1$, and other parameters as in Fig. 3. In (A-D), $D = 0.1$.

Migration introduces two competing effects. On the one hand, migration acting between communities in the same state can reduce the chances of a transition, by suppressing changes to the community's state. Indeed, in the limit of strong migration (high D) the abundances are equalized between all communities, and the meta-community behaves as a single well-mixed community, with lower effective noise (ω_i^2 reduced by a factor of $1/M$) due to the larger absolute populations of each species. On the other hand, with migration the transition can happen in only one community, and then expand to the entire meta-community. This increases the chances of transition per unit time at weaker migration levels. Due to the competition between the two effects, the mean time until the transition is a non-monotonic function of the migration rate D, see bottom panel of Fig. 5(C). Similar non-monotonic dependence was found in [24].

We showed that the state in one community is able to influence the state of communities coupled to it, such that they adopt its state. This process can be thought of as an "infection" or, when the state is a perfect copy, a "replication" process. It allows for selection at the level of the meta-community: states that are better able to replicate will be found in more communities, and in this way selected for in the population of communities. In an analogy with selection in Darwinian evolution, each patch corresponds to an individual organism in a fixed size population (the fixed number of communities). Spontaneous, noise-driven changes of a community's state are analogous to mutations. And as states with higher F-values are also better replicators, F corresponds to *fitness*. We now turn to discuss this in the full, high-diversity setting.

6 Meta-communities at high diversity: community-level selection

This section looks at meta-communities in the full, high-diversity setting. Compared to the toy model of Sec. 5, here the dynamics explore a more complex space, with many equilibria that overlap to varying degrees in their species composition. It is therefore far from obvious that intuitions from a two-state model will carry through to this case. In particular, while a community in Sec. 5 can only jump between two states, here a state might expand in an "imperfect" way, inducing similar but not identical states in neighboring communities. We find that, as in the simple model discussed in in Sec. 5, states with higher F-values are also better replicators, and so spatial expansion promotes the growth of F via a selection process.

In Fig. 6 the communities are arranged in a linear chain, as in Fig. 5(C). Fig. 6(A) shows one run. For

each time and community, the value of F is plotted, at the equilibrium associated with each community state (found by running zero-noise dynamics of the community in isolation). A number of distinct time periods can be seen. First, at $t \lesssim 10$, the communities relax into different states (see Fig 6(D)). The transitions between states then slow down and states in different communities become more similar, and by time $t = 300$, all communities assume the same state. The cross-correlation between different communities is presented in Appendix C (Fig. 11). Then there is no change until $t = 1380$ at which time all communities transition to a new state with higher F. The change occurs within a short time frame of less than 100 time units, and so looks like a jump in F in Fig. 6(B). A close-up on this time frame, Fig. 6(C), shows a front of the new state which sweeps through the chain of communities, until taking over the entire system. In the analogy with population dynamics, a new state (analogous to a mutation) has spread and fixed in the population. This expansion forms copies of exactly the same state, analogous to a replication process. This is the most common mode of change at late times, see also additional runs at higher diversity ($S = 100$) in Appendix C.

Spatial expansion leads to selection of states with higher F, as shown in Fig. 6(A,B,C). This allows $\langle F(t) \rangle$ to reach higher values than those attained for a single community ($D = 0$) at late times, see Fig. 6(E). The rate of any given transition between two states is expected to depend non-monotonically on the migration rate D, as discussed for the 3-species model in Sec. 5. This translates here to a non-monotonic dependence of $\langle F(t) \rangle$ on D, see the inset in Fig. 6(E).

7 Generality and limitations

The phenomena described above persists under many variations on the model details, and so might be found in more biologically-realistic models, and be relevant to natural or laboratory settings. Elements which do not change the behavior include (for details and simulation results see Appendix B): some fraction of pairs ij where only one of the α_{ij} is non-zero; interactions that are not of a Lotka-Volterra form (saturating interactions); niche structure, in which the pairs with non-zero interactions are chosen according to the distance in niche space; and additional interactions between all pairs, that are less competitive (not mutually-exclusive). All the phenomena described do not require very high diversity: the examples in Sec. 3-6 used $S = 24$ species, and are already present with even fewer species.

At the same time, once certain parameters are changed beyond some limit, the system dramatically changes its qualitative behavior. This includes changes which might at first sight seem innocuous or unrelated to the phenomena of interest. For example, directionality or growth of stability will be lost if the mean interaction strength is lower than some value (see Sec. 2), or if the noise is higher than some value, see Appendix B.

High-diversity communities exhibit distinct qualitative regimes, known as phases, controlled by a few driving parameters [7, 26, 39, 44–46]. Identifying these sometimes counter-intuitive parameters is key to understanding the potential behaviors of a system and the transitions between them. In these terms, the present work characterizes a distinct phase.

8 Discussion

In this work, we have looked at the dynamics of ecological communities, in which each species interacts in a mutually-exclusive way with a few others. In a meta-community, the habitats hosting the communities are fixed and connected only via migration. In order to disentangle different effects, other processes are excluded, such as evolution (leading to changes in interactions, speciation, etc.), additional community replication [47] (e.g., by host replication [16]) or external selection of entire communities [17]. The focus is on the consequences of this minimal setting, rather than on the possible biological contexts that might lead to this behavior. In this way it uncovers the crucial ingredients that might lead to similar behavior in potentially very different biological scenarios, and which indeed persist under many variations on the model details, see Sec. 7.

This minimal setting nevertheless leads to a host of remarkable phenomena. A single function of the community species' abundances governs two processes: first, this function increases during the dynamics of a single community, and so ensures directionality in its succession pattern. Secondly, this function is correlated with the ability of a community state to expand to other communities. In turn, this expansion process enhances the directionality in meta-communities, by selection of states that efficiently expand in the population of communities, in analogy with the increase in fitness due to selection in evolutionary population dynamics. Ultimately, directionality and stability within a single community, and spatial expansion, are all intimately related. Community states become a key level of organization, as much of the behavior can be described via a single number for each community state, buffering many other characteristics of the different states.

The behavior of the meta-community changes qualitatively between early and late times. At early times, it develops by a complex combination of internal changes and

cross-community influences, different facets of which can been described in multiple ways. The ability of a community to borrow features from its surroundings, and then reproduce to other communities which inherit this state, can be viewed as a Lamarkian feature [15]. A process in which a new state forms by combining the previous community state and that of its neighbors, rather than a perfect copy of a single state, has parallels with sexual reproduction [19, 48]. At late times, however, the dominant mode of change in the system starts with a jump to a new state in one community, which then replicates faithfully across the entire system, see Fig. 6(A,C) and additional examples in Appendix C. Such behavior is analogous to a mutation and replication process, with a mutation that is, a priori, directional rather than neutral. This "mutation-replication" behavior is an outcome of the dynamics, rather than a model assumption.

The growth of stability described in Sec. 3, in the sense that communities spend ever longer times at a single state or near it, means that changes occur over many different time-scales, from time scales of an individual species response to many orders of magnitude above that. The speed of changes at long time-scales depend significantly on details such as the size of the noise. In meta-communities, the dynamics might speed up significantly with the number of communities, as states which might take over are explored in parallel in the different communities. When studying systems over long time-scales, additional processes such as environmental fluctuations or evolution might become important and should be taken into account. Introducing evolution may raise interesting questions regarding multi-level selection [49], once three levels of organization–genes, organisms and communities–play an active role.

The work raises a number of interesting directions for future research. Firstly, while we have proposed some intuitive explanations for the observed phenomena, a deeper theoretical understanding is called for, with the goal of understanding the entire dynamics within a single coherent picture. Why does the function F increase, and what is its functional form? Can a quantitative description be constructed at the level of the F-values of states alone, without reference to additional details? For example, how well does the F-value of a given state predict its ability to expand, and why?

It would be interesting to further explore the conditions for these phenomena to hold. For example, mutually exclusive pairs might be replaced by groups of species that compete in a more structured interaction pattern. In the present work, the interactions are predominantly competitive. Can similar models be constructed for strong (obligate) mutualism, an important driver of close associations between species [14, 15]?

Acknowledgments – The research was supported by the Israel Science Foundation (ISF) Grant no. 773/18.

References

[1] Eugene P. Odum. The Strategy of Ecosystem Development. *Science*, 164:262–270, 1969.

[2] S. P. Hubbell. *The unified theory of biogeography and biodiversity*. University Press, Princeton, 2001.

[3] Elisa Benincà, Jef Huisman, Reinhard Heerkloss, Klaus D. Jöhnk, Pedro Branco, Egbert H. Van Nes, Marten Scheffer, and Stephen P. Ellner. Chaos in a long-term experiment with a plankton community. *Nature*, 451(7180):822–825, February 2008.

[4] Jef Huisman and Franz J Weissing. Biodiversity of plankton by species oscillations and chaos. *Nature*, 402(6760):407–410, 1999.

[5] Andrea Belgrano, Ursula M. Scharler, Jennifer Dunne, Robert E. Ulanowicz, and Ulrich Brose. *Aquatic Food Webs*. Oxford University Press, April 2005.

[6] Michael Doebeli, Yaroslav Ispolatov, and Burt Simon. Towards a mechanistic foundation of evolutionary theory. *eLife*, 6, February 2017.

[7] Sigurd Diederich and Manfred Opper. Replicators with random interactions: A solvable model. *Physical Review A*, 39(8):4333, 1989.

[8] Tobias Galla and J. Doyne Farmer. Complex dynamics in learning complicated games. *Proceedings of the National Academy of Sciences*, 110(4):1232–1236, January 2013.

[9] L. J. McCook. Understanding ecological community succession: Causal models and theories, a review. *Vegetatio*, 110(2):115–147, February 1994.

[10] Brian D. Fath, Bernard C. Patten, and Jae S. Choi. Complementarity of Ecological Goal Functions. *Journal of Theoretical Biology*, 208(4):493–506, February 2001.

[11] Robert Mac Arthur. Species packing, and what competition minimizes. *Proceedings of the National Academy of Sciences*, 64(4):1369–1371, 1969.

[12] Robert MacArthur. Species packing and competitive equilibrium for many species. *Theoretical Population Biology*, 1(1):1–11, May 1970.

[13] Frederic Edward Clements. *Plant succession: an analysis of the development of vegetation*. Number 242. Carnegie Institution of Washington, 1916.

[14] Thomas C.G. Bosch and Margaret J. McFall-Ngai. Metaorganisms as the new frontier. *Zoology*, 114(4):185–190, September 2011.

[15] Seth R. Bordenstein and Kevin R. Theis. Host Biology in Light of the Microbiome: Ten Principles of Holobionts and Hologenomes. *PLOS Biology*, 13(8):e1002226, August 2015.

[16] Joan Roughgarden, Scott F. Gilbert, Eugene Rosenberg, Ilana Zilber-Rosenberg, and Elisabeth A. Lloyd. Holobionts as Units of Selection and a Model of Their Population Dynamics and Evolution. *Biological Theory*, 13(1):44–65, March 2018.

[17] David Sloan Wilson. Complex Interactions in Metacommunities, with Implications for Biodiversity and Higher Levels of Selection. *Ecology*, 73(6):1984–2000, December 1992.

[18] M. Gilpin. Community-level competition: asymmetrical dominance. *Proceedings of the National Academy of Sciences*, 91(8):3252–3254, April 1994.

[19] Mikhail Tikhonov. Community-level cohesion without cooperation. *Elife*, 5:e15747, 2016.

[20] Marten Scheffer, Jordi Bascompte, William A. Brock, Victor Brovkin, Stephen R. Carpenter, Vasilis Dakos, Hermann Held, Egbert H. van Nes, Max Rietkerk, and George Sugihara. Early-warning signals for critical transitions. *Nature*, 461(7260):53–59, September 2009.

[21] Egbert H. van Nes and Marten Scheffer. Implications of spatial heterogeneity for catastrophic regime shifts in ecosystems. *Ecology*, 86(7):1797–1807, July 2005.

[22] Golan Bel, Aric Hagberg, and Ehud Meron. Gradual regime shifts in spatially extended ecosystems. *Theoretical Ecology*, 5(4):591–604, November 2012.

[23] Daniel R. Amor, Raúl Montañez, Salva Duran-Nebreda, and Ricard Solé. Spatial dynamics of synthetic microbial mutualists and their parasites. *PLOS Computational Biology*, 13(8):e1005689, August 2017.

[24] Seyfullah Enes Kotil and Kalin Vetsigian. Emergence of evolutionarily stable communities through eco-evolutionary tunnelling. *Nature Ecology & Evolution*, 2(10):1644–1653, October 2018.

[25] Jean-Francois Arnoldi, Sylvain Coq, Sonia Kefi, and Sebastien Ibanez. Tannin evolution by niche construction: a spatial stoichiometric model. *bioRxiv*, page 320572, 2018.

[26] Guy Bunin. Ecological communities with lotka-volterra dynamics. *Physical Review E*, 95(4):042414, 2017.

[27] Giulio Biroli, Guy Bunin, and Chiara Cammarota. Marginally stable equilibria in critical ecosystems. *New Journal of Physics*, 20(8):083051, August 2018.

[28] Yael Fried, Nadav M. Shnerb, and David A. Kessler. Alternative steady states in ecological networks. *Physical Review E*, 96(1), July 2017.

[29] Yael Fried, David A. Kessler, and Nadav M. Shnerb. Communities as cliques. *Scientific Reports*, 6:35648, October 2016.

[30] Haim Sompolinsky, Andrea Crisanti, and Hans-Jurgen Sommers. Chaos in random neural networks. *Physical Review Letters*, 61(3):259, 1988.

[31] Leticia F. Cugliandolo, Jorge Kurchan, Pierre Le Doussal, and Luca Peliti. Glassy behaviour in disordered systems with nonrelaxational dynamics. *Physical review letters*, 78(2):350, 1997.

[32] Ludovic Berthier, Jean-Louis Barrat, and Jorge Kurchan. A two-time-scale, two-temperature scenario for nonlinear rheology. *Physical Review E*, 61(5):5464, 2000.

[33] Martin L. Cody, Robert H. MacArthur, and Jared M. Diamond. *Ecology and evolution of communities*. Harvard University Press, 1975.

[34] Timothy H Keitt, Mark A Lewis, and Robert D Holt. Allee effects, invasion pinning, and species' borders. *The American Naturalist*, 157(2):203–216, 2001.

[35] S. E. Bayley, I. F. Creed, G. Z. Sass, and A. S. Wong. Frequent regime shifts in trophic states in shallow lakes on the Boreal Plain: Alternative "unstable" states? *Limnology and Oceanography*, 52(5):2002–2012, September 2007.

[36] Erik S. Wright and Kalin H. Vetsigian. Inhibitory interactions promote frequent bistability among competing bacteria. *Nature Communications*, 7(1), December 2016.

[37] Jason D. Moll and Joel S. Brown. Competition and Coexistence with Multiple Life-History Stages. *The American Naturalist*, 171(6):839–843, June 2008.

[38] Yu A. Pykh. Lyapunov functions for Lotka-Volterra systems: an overview and problems. In *Proceedings of the Fifth IFAC Symposium on Nonlinear Control Systems*, pages 1655–1660, 2001.

[39] David A Kessler and Nadav M Shnerb. Generalized model of island biodiversity. *Physical Review E*, 91(4):042705, 2015.

[40] Marten Scheffer, Steve Carpenter, Jonathan A. Foley, Carl Folke, and Brian Walker. Catastrophic shifts in ecosystems. *Nature*, 413(6856):591–596, October 2001.

[41] Ludovic Berthier and Giulio Biroli. Theoretical perspective on the glass transition and amorphous materials. *Reviews of Modern Physics*, 83(2):587–645, June 2011.

[42] Daniel J. Amit, Hanoch Gutfreund, and H. Sompolinsky. Spin-glass models of neural networks. *Physical Review A*, 32(2):1007–1018, August 1985.

[43] Michel Loreau. *From populations to ecosystems: theoretical foundations for a new ecological synthesis (MPB-46)*, volume 52. Princeton University Press, 2010.

[44] Charles K Fisher and Pankaj Mehta. The transition between the niche and neutral regimes in ecology. *Proceedings of the National Academy of Sciences*, 111(36):13111–13116, 2014.

[45] Mikhail Tikhonov and Remi Monasson. Collective Phase in Resource Competition in a Highly Diverse Ecosystem. *Physical Review Letters*, 118(4), January 2017.

[46] Matthieu Barbier, Jean-François Arnoldi, Guy Bunin, and Michel Loreau. Generic assembly patterns in complex ecological communities. *Proceedings of the National Academy of Sciences*, 115(9):2156–2161, February 2018.

[47] Arne Traulsen and Martin A. Nowak. Evolution of cooperation by multilevel selection. *Proceedings of the National Academy of Sciences*, 103(29):10952–10955, 2006.

[48] Michael J. Rosen, Michelle Davison, Devaki Bhaya, and Daniel S. Fisher. Fine-scale diversity and extensive recombination in a quasisexual bacterial population occupying a broad niche. *Science*, 348(6238):1019–1023, May 2015.

[49] David Sloan Wilson and Elliott Sober. Reviving the superorganism. *Journal of Theoretical Biology*, 136(3):337–356, February 1989.

[50] A. Steger and N. C. Wormald. Generating Random Regular Graphs Quickly. *Combinatorics, Probability and Computing*, 8(4):377–396, July 1999.

[51] Mark EJ Newman and Michelle Girvan. Finding and evaluating community structure in networks. *Physical review E*, 69(2):026113, 2004.

Appendix A. Model definition and simulations

We first define the basic variant of the model, used in the main text. For convenient reference, all parameters used all simulations are concentrated here, including those quoted in the main text.

The interaction matrix α in the model used in the main text, Sec. 2,3,4,6, is constructed by first sampling a network of non-zero interactions. It is taken to be a random regular graph, i.e. where each species interacts with C other species, generated using the algorithm in [50]. For a pair of species i, j that interact, both the interactions α_{ij}, α_{ji} are non-zero and sampled independently from a Gaussian distribution.

The parameters are as follows: In Fig. 2(A), $C = 20, \mathrm{std}\left(\alpha_{ij}\right) = 0.4, S = 400$, and all $r_i = 1$. In Fig. 3,4 and 6, $C = 3, \mathrm{mean}\left(\alpha_{ij}\right) = 1.667, \mathrm{std}\left(\alpha_{ij}\right) = 0.75, S = 24$. The growth rates r_i were sampled independently for each i, from a uniform distribution on $[0.5, 2]$. Everywhere, $\lambda_i = 10^{-5}$ for all i. The noise amplitude is $\omega_i = 0.173$ for all i in Fig. 3,4. In Fig. 6, $\omega_i = 0.1$ and $D = 0.1$. Initial conditions for $N_i\left(0\right)$ are uniform on $[0, 1]$.

The $S = 2$ models in Fig. 2, have $\alpha_{12} = 4, \alpha_{21} = 2$ in (B) and $\alpha_{12} = 0.6, \alpha_{21} = 0.4$ in (C). The 3-species model shown in Fig. 5 is defined by $\alpha_{12,21,13,31} = 1.5, \alpha_{23,32} = 0, \omega_i = 0.173, r_i = 1$ and $D = 0.03$.

Zero-noise dynamics shown in Fig. 2 are simulated with migration rate $\lambda = 10^{-15}$, using a Runge-Kutta ordinary differential equation solver, with relative and absolute error tolerance of 10^{-13}.

Noisy dynamics are integrated by a standard stochastic differential equation algorithm. The abundances $N_i\left(t\right)$ are advanced by

$$N_i\left(t + \Delta t\right) = N_i\left(t\right) + A_i\left(\overrightarrow{N}\right)\Delta t + B_i\left(\overrightarrow{N}\right)\sqrt{\Delta t}\eta_i \,,$$

where $A_i\left(\overrightarrow{N}\right)$ is the deterministic term in the right-hand side of Eq. (1,4), and $B_i\left(\overrightarrow{N}\right) = \omega_i\sqrt{N_i}$ is the prefactor of the white noise, and η_i is a Gaussian with unit variance and zero mean. We take $\Delta t = 0.01$. If some $N_i\left(t + \Delta t\right)$ goes below 10^{-10}, it is set to 10^{-10} (with $\lambda = 10^{-5}$ used in all stochastic simulations, this doesn't happen often). A different regularization, $B_i\left(\overrightarrow{N}\right) = \omega_i\sqrt{N_i + \lambda}$, has also been tested and gives very similar results.

Correlations between two abundances at two times, $\overrightarrow{N}\left(t_1\right), \overrightarrow{N}\left(t_2\right)$, in one community are calculated by first

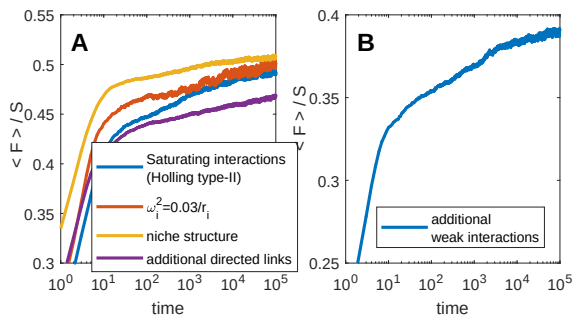

Figure 7: $\langle F\left(t\right)\rangle$ for different model variants. Full definitions and parameters values are given in the text.

recording

$$C_1\left(t_1, t_2\right) \equiv \left[\frac{1}{S}\sum_i N_i\left(t_1\right)N_i\left(t_2\right)\right]_{noise} - \left[\frac{1}{S}\sum_i N_i\left(t_1\right)\right]_{noise}\left[\frac{1}{S}\sum_i N_i\left(t_2\right)\right]_{noise} ,$$

where $\left[..\right]_{noise}$ denotes the average over noise realizations with the same initial conditions and α_{ij}, r_i, where 10 repetitions with different noise realizations are used. Averaging $C_1\left(t, t'\right)$ over model samples $\left(\alpha_{ij}, r_i\right)$ and initial conditions gives $C_{u.n.}\left(t, t'\right)$. Finally, the correlation coefficient shown in the main text is given by: $C\left(t, t'\right) \equiv C_{u.n.}\left(t, t'\right)/\sqrt{C_{u.n.}\left(t, t\right)C_{u.n.}\left(t', t'\right)}$. In metacommunities, the correlations for different communities are computed similarly, only with $\overrightarrow{N}^{(u_1)}\left(t_1\right), \overrightarrow{N}^{(u_2)}\left(t_2\right)$ where u_1, u_2 represent different communities, and the sum over i is replaced by a sum over i and all $u_1 \neq u_2$.

Appendix B. Variants of the basic model

The main properties discussed in the main text are insensitive to many of the model's details. We now discuss a number of variants of the basic model. For all of them we show $\langle F\left(t\right)\rangle$, the equivalent of the smooth line in Fig. 3(B). For five variants of the model, we show that $\langle F\left(t\right)\rangle$ continues to increase over long times, roughly as $\langle F\left(t\right)\rangle \propto \ln t$, as in the basic variant of the model used in the main text.

At the same time there are phase boundaries that, when crossed, may change the behavior significantly, as in the transition from directionality to chaos upon changing $\langle\alpha_{ij}\rangle$ discussed in Sec 2, see Fig. 2. Below we also give another example of such a transition, when the noise is increased beyond some value.

The basic model variant used in the main text has a number of mutually-exclusive pairs of interactions per species. Other interaction-types may be present too. Already in the basic model (Figs. 3,4 and 6), 66% of the the non-zero interaction pairs are mutually-exclusive (both $\alpha_{ij}, \alpha_{ji} > 1$), 30% have just one $\alpha_{ij} > 1$, and the rest may coexist in pairs ($\alpha_{ij}, \alpha_{ji} < 1$). In a first variant, we look at graphs where 15% of the interactions are directional, such that one of the interactions is non-zero ($\alpha_{ij} > 0$ with $\alpha_{ji} = 0$). This is done by creating a random regular graph (undirected) with $C = 3$ links per species and another directed graph in which each species i has 3 j-values for which α_{ij} is non-zero ($j = i$ allowed). Then, edges from the former network are taken with probability 0.85 and from the latter with probability 0.15 (this also reduces the fraction of non-zero mutually-exclusive pairs to 57%). Running simulations with these interactions shows a similar behavior of $\langle F(t) \rangle$, see Fig. 7(A), "additional directed links". (Other model parameters: $S = 24, \text{mean}(\alpha_{ij}) = 1.667, \text{std}(\alpha_{ij}) = 0.58, \omega_i = 0.173$, r_i uniform on $[0.5, 2]$).

In another variant, interactions are taken to have a non-linear form,

$$\frac{dN_i}{dt} = r_i N_i \left[1 - \sum_{j=1}^{S} \alpha_{ij} g(N_j) \right]$$

with a saturating Holling type-II function for the interactions, $g(N) = \frac{N}{1+cN}$. This requires a different formula for the growing function F. Indeed, in the case where the matrix α is symmetric, the Lyapunov function generalizes straight forwardly to [38]

$$F\left(\vec{N}\right) = 2\sum_{i=1}^{S} r_i g(N_i(t)) - \sum_{i,j=1}^{S} r_i \alpha_{ij} g(N_i(t))\, g(N_j(t)) \ .$$

The behavior of $\langle F(t) \rangle$ with this function also increases approximately logarithmically, see Fig. 7(A), "saturating interactions". (Model parameters: $S = 24, C = 3, \text{mean}(\alpha_{ij}) = 1.667, \text{std}(\alpha_{ij}) = 0.58, \omega_i = 0.173$, and $c = 1$, r_i uniform on $[0.5, 2]$).

Another variant regards the network of non-zero interactions. In the basic model it is sampled as a random regular graph, with 3 links per species. Here we sample it from an underlying niche structure. The different species are embedded in a two-dimensional niche space, in which each species' location is a point sampled uniformly in the square $(0,1) \times (0,1)$. Two different species are assigned a non-zero interaction if the distance between them is smaller than d_0. We choose $d_0 = 0.23$, so that the *average* number of non-zero pairs is about 3, but this number fluctuates significantly between species. Moreover, this construction gives the interaction network additional structure beyond a random regular graph. For example, the network has some degree of modularity [51]: if species i, j are close in niche space so as to interact, as are species j, k, then it is more likely that species i, k are close enough to interact. With this structure, the logarithmic growth is still observed, see Fig. 7(A), "niche structure".

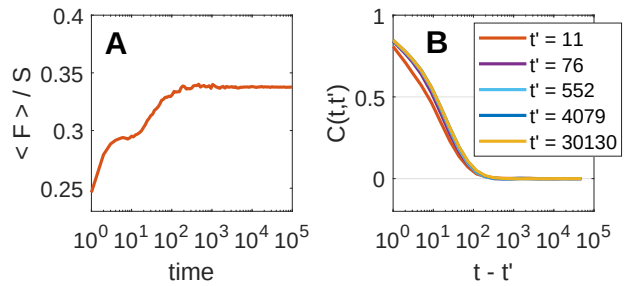

Figure 8: The equivalent of Fig. 3(B,C) in the same model, only with larger noise ($\omega_i = 0.4$). (A) The function $\langle F(t) \rangle$ increases at first but saturates and does not increase at long times. (B) The correlation $C(t, t')$ decays after shorter times ($t - t' \sim 10^2$) and for late times depends only on the time difference $t - t'$, as shown by same behavior for $t' = 4079, 30130$. These results mean that here there is no slow-down of the dynamics, that could come from transitions towards states with ever higher stability.

Another change involves having noise amplitudes ω_i that are dependent on i. If these are random numbers that are not correlated with any other system parameters, little changes in the behavior. Interestingly, the logarithmic growth survives even if ω_i has some relation to r_i, here tested for $\omega_i^2 = 0.03/r_i$, see Fig. 7(A) (Parameters: $S = 24, C = 3, \text{mean}(\alpha_{ij}) = 1.667, \text{std}(\alpha_{ij}) = 0.75$, r_i uniform on $[0.5, 2]$).

Finally, we demonstrate the effect of additional weaker interactions in all pairs. The model takes the interactions in the basic model $S = 24, C = 3, \text{mean}(\alpha_{ij}) = 1.667, \text{std}(\alpha_{ij}) = 0.75$, and adds to them non-zero interactions to all pairs $i \neq j$, sampled independently from $P(\alpha_{ij}) = e^{-\alpha_{ij}/0.04}$, so that the mean of the additional terms is 0.04. Note that while individually these numbers are small compared to the nominal interactions, they appear for *all* interactions pairs, rather than just for $C = 3$ links per species. Here too $\langle F \rangle$ grows over long time scales, see Fig. 7(B).

For comparison, it is instructive to see an example that shows a different behavior. Here we look at a system exactly like that in Fig. 3,4 and 6, only with higher noise, $\omega_i = 0.4$ (instead of 0.173), see Fig. 8. The function $\langle F(t) \rangle$ grows but saturates at times $t \sim 100$, and does not show a subsequent logarithmic growth (in contrast to Fig. 3(B)). Together with that, the correlation $C(t, t')$

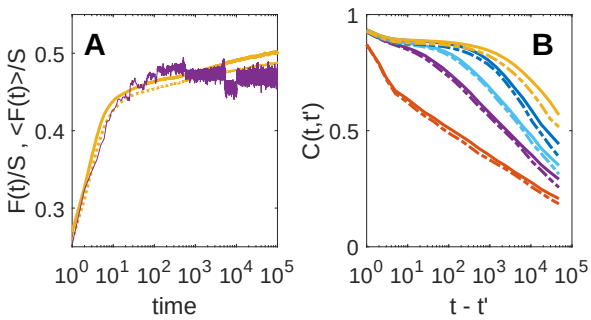

Figure 9: (A) $\langle F(t)\rangle$ for $S = 100$ (thick solid line), compared with the same for $S = 24$ (dotted line), as in Fig. 3(B). A single example run for $S = 100$ is shown. (B) The two-time correlation $C(t, t')$ for $S = 100$ (solid lines) and $S = 24$ (dotted lines). Line of different colors show different t' values, as in Fig. 3(C).

from time t' to t decays more quickly (compare with Fig. 3(C)). Crucially, at later times t' it depends only on the time difference $t - t'$, i.e. $C(t, t') = f(t - t')$, as seen in the almost identical dependence on $t - t'$ of the correlations starting at $t' = 4079, 30130$.

While growth of $F(t)$ implies reaching a fixed point, the converse is not generally true. For example, a fixed point is reached in Fig. 2(B,C) but $F(t)$ decreases on the way, and similarly for high S dynamics discussed in [26], in which a fixed-point is reached.

Appendix C. Higher diversity and correlations between communities

In this section the results at two different diversities S are compared. It also shows the cross-correlation between communities, not shown in the main text.

As the number of species S is increased, the mean $\langle F(t)\rangle / S$ converges to a function, quite close to the the one for $S = 24$, see the comparison with $S = 100$ in Fig. 9(A). Individual runs with higher S follow the mean $\langle F(t)\rangle$ more closely, and have more transitions between states, see example in Fig. 9(A). The two-time correlation $C(t, t')$ converges to a well-defined limit as S grows, so the increase in the number of transitions does not induce a faster decorrelation; Again, the function for $S = 24$ is quite close to the asymptotic function. For any S (as for $S = 24$), the rate of transitions between states strongly decreases with time, and so even at higher diversity there is a time after which the system spends extended periods of time in a given state, punctuated by transitions to new states.

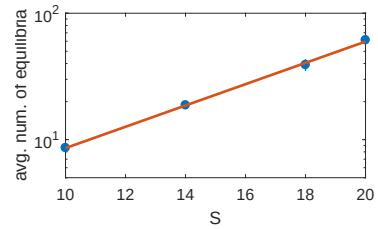

Figure 10: Average number of stable equilibria as a function of S. Solid line: fit to exponential, $e^{0.194 \cdot S + 0.209}$.

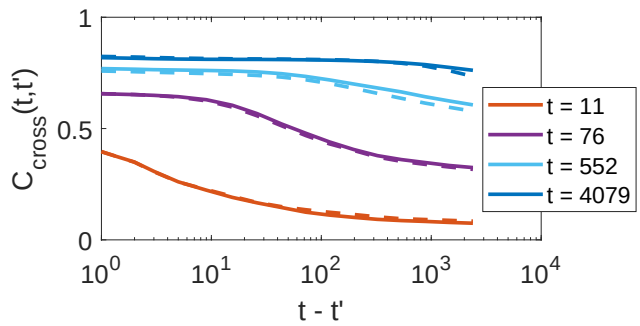

Figure 11: Cross-correlation between neighboring communities in a chain of $M = 10$ communities as in Fig. 6. Comparison between $S = 100$ (solid lines) and $S = 24$ (dashed lines).

The number of equilibria increase with S, see Fig. 10. They are counted by exhaustively checking all subsets of species for equilibria. The dependence fits well to an exponential between $S = 10$ to 20, as was shown for a related, more stylized model [28]. This predicts that at $S = 24$ there will be on average about 130 states, and for $S = 100$ about $3 \cdot 10^8$ states.

Cross correlation between neighboring communities in a meta-community are shown in Fig. 11. Parameters are the same as for Fig. 6, with $D = 0.1$. The correlation between nearby communities is less than one even if the communities are fluctuating in the same state, because they experience different demographic noise in each community. Results for $S = 24, 100$ are shown, and again found to be very similar.

It is interesting to note that the spread of states through the meta-community causes any given community to experience more changes of state, as the new states can be created in any community before spreading. To test this, we looked the state of one community within the meta-community, at $S = 24$, at times $30, 100, 300, 10^3, 3 \cdot 10^3, 10^4$, in repeated runs with parameters as in Fig. 6(A). The number of changes of states between subsequent times was on average larger by $43\%_{(\pm 3\%)}$ than for a single isolated community.

Additional run samples – Fig. 12 shows 4 runs sam-

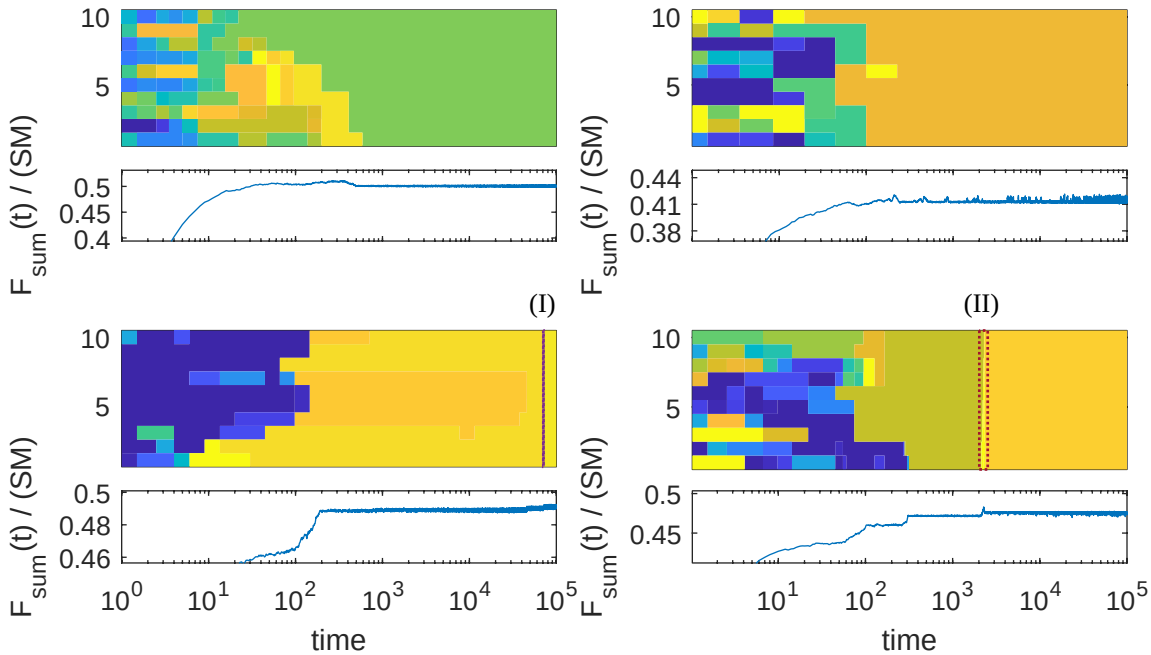

Figure 12: Additional run samples, with the same model parameters as Fig. 6(A-D) except for $S = 100$. For each run the map of states is shown as in Fig. 6(A), and below each $F(t)/(SM)$ is plotted as in Fig. 6(B). In order to show difference at late times, the colors do not differentiate all the early states with low F-values.

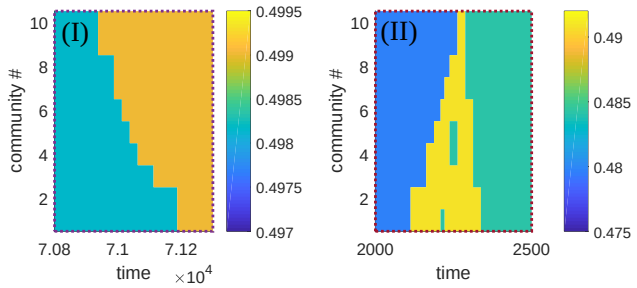

Figure 13: Close-up on two areas in Fig. 12. For clarity, colors have been changed from Fig. 12.

pled as in Fig. 6(A), except for $S = 100$ here. The four runs are an unbiased sample–without any additional selection by the author. Fig. 13 shows a close up on two areas in Fig. 12, showing sweeps in which a new state takes over the system. Fig. 12(II) shows two consecutive sweeps; in the later a state with somewhat lower F takes over.